ACTIVE CONTROL ON TYPICAL HELICOPTER PANELS BY USING PIEZO-ACTUATORS

L. De Vivo, A. Concilio

C.I.R.A. S.C.p.A. (Italian Aerospace Research Center)
Via Maiorise, loc. Silvagni 81043 Capua-CE, ITALY

Abstract

To evaluate the feasibility and the performance of an active control system based on the use of piezoceramic patches, is necessary to develop suitable "Strain Actuation" (S.A.) models, able of describing the interaction between the structure and the actuators. This is necessary for elements that present a little background of previous experiences: such is the case for sandwich and composite helicopter panels. This paper reports a review of the most commonly used 1D and 2D numerical and analytical models of the strain transmission phenomenon, with an extension to general composite materials. Two applications are then shown: a first, relative to a flat honeycomb plate, as designed and manufactured by ONERA, Toulouse, clamped on the 4 sides; a second, on a curved composite panel designed and manufactured by DASA, Munich, made of a trim and a skin part, connected by stringers unsymmetrically placed. Results show a good agreement between the numerical prediction and the available experimental data, as well as the good performance of the simulated control systems. In the end, a possible index of the actuators placement quality, is also defined.

Introduction

To evaluate the feasibility of a control system based on the use of piezoelectric materials as sensors and/or actuators, it is necessary to evaluate the effectiveness os such devices.[1][2] This is particularly important for structures that have not been investigated in this field before or present a little background of previous experiences; such is the case for sandwich and composite helicopter panels.
Such a research refers to the new discipline known as "Smart Materials and Structures".[3][4] Authors have worked on such subject for a long time, on applications dedicated to turbo-prop aircraft,[5][6] and expanding the results on helicopter structures in this last period,[7] inside the Brite EuRam project RHINO[8] (Research on Helicopter Interior Noise), just concluded with interesting results. Three main kinds of active noise control strategies may be currently highlighted:

- action on the vibration by information acquired on the structure;[9]
- action on the acoustic field by information acquired on the interior noise;[10][11]
- action on the structure by information acquired on the sound field.[12]

The first is based on the simple concept that, because at low frequencies the interior noise is mainly produced by the structural vibration, to reduce the vibration field should cause a sound level reduction. The second idea is simple as well: it aims at reducing the noise field directly, regardless of the structural behaviour. Recent studies showed that another way can be successfully run to minimise interior noise levels: the so-called modal re-shaping of the dynamic structural response.[13] Moreover, the first applications of "direct noise control" (system based on microphones as sensors, and loudspeakers as actuators) was not entirely satisfying: the high-level of vibration inside the cabin, left untouched by the active noise control, caused some passengers to suffer a strange situation of no-noise and high vibration, so that they declared the non-controlled condition as preferable.[11][14]
The last way seems to be the most promising; apart of the previous considerations, it has to be stressed that in this case both the two different strategies of "modal suppression" (direct vibration reduction) or "modal restructuring" (modifying the dynamic deformed shape) are implicitly applied. In fact,

the measure of the noise field is chosen as cost function , so that the actuators try "automatically" to force a structural response characterised by the lowest internal radiation, as well as to reduce itself.
This paper reports a first step made on the way of reducing noise in helicopter cabins by "smart devices". It has been divided into three parts: the first contains a summary of the most common analytical-numerical S.A. models used to simulate the action of piezoactuators. Two different specimens are examined: a flat honeycomb (realised at ONERA, Touluse, F) and a curved composite plate (realised by Daimler Benz laboratory in Ottobrunn, D). In particular, the chosen objective functions were the sound power radiation and the vibrational energy, respectively.
For the aforesaid reasons, to investigate both these aspects is necessary. Comfort index has to be forecast as a combination of vibrational and acoustic levels, so that efforts in both directions are to be provided. This aspect is beyond the scope of this article, but a great deal of studies are on-going, letting preview a further expansion on the subject, really important for the definition of the control system objective.

Strain actuation models

The S.A. model proposed by Crawley,[1] demonstrated the main influence of the bonding layer in the force transmission process from a piezo to a structural element. Moreover, it revealed as its action could be considered as concentrated at the boundaries of the contact region. Starting from these results, obtained on a unidimensional structure, bi-dimensional models were realised.
In particular,[16] the extension of the analytical idealisation was performed by assuming Poisson's moduli in both piezo and structure materials equal to 1/3 (a common case in practice). Dimitriadis et al.,[2] assuming the piezoactuators perfectly bonded to the structure, found a general 2D formula describing the S.A. phenomena.

Isotropic panel

Concilio[17] proposed a similar model; but starting from slight different assumptions. Particularly, by considering (fig.1):

- two bending actuators perfectly bonded on the structure[1];
- linear strain along the piezo and the structural thickness, with the same slope (the main difference with the formulation given by Dimitriadis et al.)[2];
- the transmitted forces acting on the contact region boundaries.

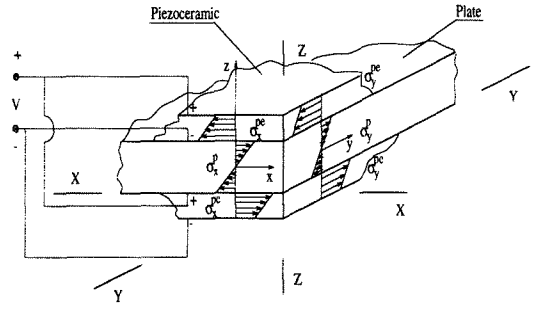

FIGURE 1: *Stress distribution due to piezo's action*

the transmitted strain could be found:

$$\varepsilon_t = f_\varepsilon \cdot \Lambda \tag{1}$$

where f_ε is a reduction factor, expressed as:

$$f_\varepsilon = \frac{6(\overline{T} + \overline{T}^2)}{E_\nu + 6\overline{T} + 12\overline{T}^2 + 8\overline{T}^3} \tag{2}$$

$\overline{T}$ is the ratio between the piezo, T_p, and the structural thickness, T_s, and E_ν is equal to $E_s/E_p \cdot (1-\nu_p)/(1-\nu_s)$. Transmitted stress, forces and moments per unit of length can be calculated by considering the classical expressions:

$$\sigma_t = \frac{E_s}{1-\nu_s} \cdot f_\varepsilon \cdot \Lambda = f_\varepsilon \cdot \sigma_{id} \tag{3}$$

$$F_t = \frac{E_s}{1-\nu_s} \cdot \frac{T_s}{6} \cdot f_\varepsilon \cdot \Lambda = f_F \cdot F_{id} \tag{4}$$

$$M_t = \frac{E_s}{1-\nu_s} \cdot \frac{T_s^2}{6} \cdot f_\varepsilon \cdot \Lambda = f_M \cdot M_{id} \tag{5}$$

where the suffix *id* is used to define the stress, force and moment that would appear if the piezo were considered ideally clamped on the structure (maximum stress transmitted; no strain all along its thickness). To express both f_M and M_{id} may be interesting. By taking into account the expressions 1, 2 and 5 and dividing and multiplying by $E_p/(1-\nu_p) \cdot T_p \cdot (T_p + T_s)$, it follows:

$$M_t = \frac{E_\nu}{E_\nu + 6\overline{T} + 12\overline{T}^2 + 8\overline{T}^3} \cdot \frac{E_p T_p (T_s + T_p)}{1-\nu_p} \cdot \Lambda \tag{6}$$

It is easy to recognise the second term as the ideal momentum, that is to say what is generated by a piezo under a voltage V if it is

constrained to have no strain inside. Hence, the following expressions hold:

$$f_M = \frac{E_\nu}{E_\nu + 6\overline{T} + 12\overline{T}^2 + 8\overline{T}^3} \tag{7}$$

and

$$M_{id} = \frac{E_p}{1-\nu_s} \cdot T_p \cdot (T_s + T_p) \cdot \Lambda \tag{8}$$

Regarding F_{id}, an abstraction should be made: it is defined as the force able to give a transmitted moment equal to M_{id}, when it is applied on the contact surface. Then,

$$F_{id} = \frac{E_p}{1-\nu_s} \cdot T_p \cdot \frac{T_s + T_p}{T_s} \cdot \Lambda = \frac{E_p}{1-\nu_s} \cdot T_p \cdot (1+\overline{T}) \cdot \Lambda \tag{9}$$

From the expressions 4, 5 and 9 the above equality holds:

$$f_F = f_M \tag{10}$$

In figs.2 $\rightarrow$ 5, the transmitted strain and moment as a function of $\overline{T}$ or its inverse, are reported.

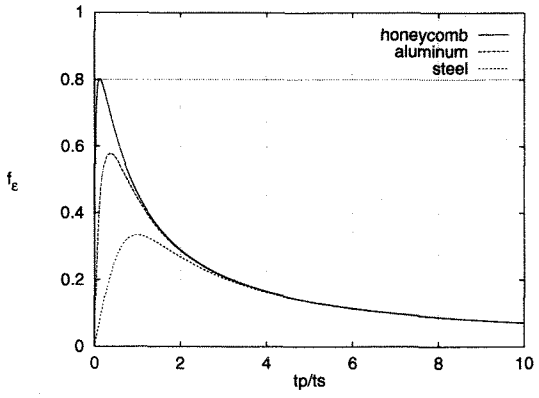

FIGURE 2: *Strain transmission factor*

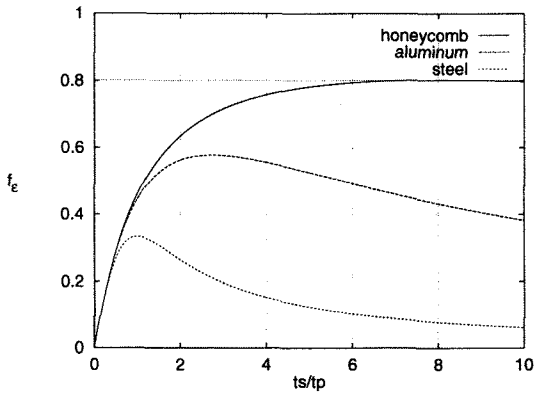

FIGURE 3: *Strain transmission factor*

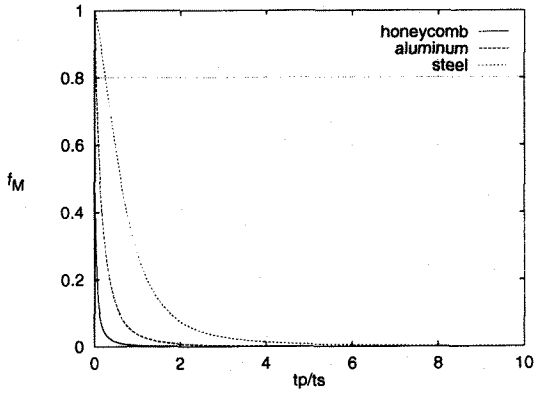

FIGURE 4: *Moment transmission factor*

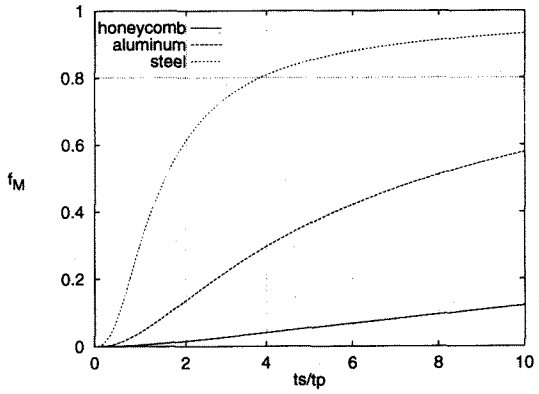

FIGURE 5: *Moment transmission factor*

While f_ε is really a measure of the strain that is transmitted to the structure, f_M is a "relative" measure, because M_{id} itself is a function of T_p and T_s. Therefore, it can be considered as a measure of the utilisation level of the piezo actuator; it has sense, anyway, to compare the curves at the same values of the thicknesses ratio for different materials.

Composite panel

The aforesaid model holds if the plate is isotropic. Otherwise, to calculate strain transmission in general honeycomb or composite structural elements, a more complex formulation should be followed, based on the classical lamination theory.[18]
Under the classical Kirchhoff thin plate theory assumptions, the equilibrium of a plate element under an arbitrary load (**N**,**M**) is regulated by the following expressions:

$$\begin{aligned} \mathbf{N} &= \mathbf{A}\varepsilon_0 + \mathbf{B}\varepsilon_1 \\ \mathbf{M} &= \mathbf{B}\varepsilon_0 + \mathbf{D}\varepsilon_1 \end{aligned} \tag{11}$$

where **A** is the extensional, **D** the bending, **B** the coupled bending-extensional stiffness, ε_0 the mid-plane strain term and ε_1 the curvature component (linear strain "hypothesis"). If a piezo actuator is subject to a voltage load, the internal stress field is given by:

$$\sigma_p = \mathbf{E_p}(\varepsilon_p - \Lambda) \tag{12}$$

where $\mathbf{E_p}$ is the stiffness matrix of the plate and Λ the strain actuation vector.
If $\mathbf{N_p}$ and $\mathbf{M_p}$ are the resulting forces at the extremities of the piezo actuator, representing the action of the structure upon it, the equilibrium will require that:

$$\begin{aligned} \mathbf{N} &= -\mathbf{N_p} \\ \mathbf{M} &= -\mathbf{M_p} \end{aligned} \tag{13}$$

where $\mathbf{N_p}$ and $\mathbf{M_p}$ are given by:

$$\begin{aligned} \mathbf{N_p} &= \int_h^{h+t_p} \sigma_p \, dz \\ \mathbf{M_p} &= \int_h^{h+t_p} \sigma_p z \, dz \end{aligned} \tag{14}$$

After integration we have:

$$\begin{aligned} \mathbf{N_p} &= \mathbf{A_p}(\varepsilon_0 - \Lambda) + \mathbf{B_p}\varepsilon_1 \\ \mathbf{M_p} &= \mathbf{B'_p}(\varepsilon_0 - \Lambda) + \mathbf{D_p}\varepsilon_1 \end{aligned} \tag{15}$$

Combining equations 11, 13 and 15 it results:

$$\begin{bmatrix} \mathbf{A} & \mathbf{B} \\ \mathbf{B} & \mathbf{D} \end{bmatrix} \begin{Bmatrix} \varepsilon_0 \\ \varepsilon_1 \end{Bmatrix} + \begin{bmatrix} \mathbf{A_p} & \mathbf{B_p} \\ \mathbf{B'_p} & \mathbf{D_p} \end{bmatrix} \begin{Bmatrix} \varepsilon_0 \\ \varepsilon_1 \end{Bmatrix} = \begin{Bmatrix} \mathbf{A_p} \\ \mathbf{B'_p} \end{Bmatrix} \Lambda \tag{16}$$

where:

- $\mathbf{A_p} = \mathbf{E_p} T_p$
- $\mathbf{B_p} = \mathbf{E_p} T_p (1 + \frac{T_p}{T_s})$
- $\mathbf{B'_p} = \mathbf{E_p} T_p^2 (\frac{1}{2} + \frac{T_s}{2T_p})$
- $\mathbf{D_p} = \mathbf{E_p} T_p^2 (1 + \frac{T_s}{2T_p} + \frac{2T_s}{3T_p})$.

The strain is then given by:

$$\begin{Bmatrix} \varepsilon_0 \\ \varepsilon_1 \end{Bmatrix} = \begin{bmatrix} \mathbf{A} + \mathbf{A_p} & \mathbf{B} + \mathbf{B_p} \\ \mathbf{B} + \mathbf{B'_p} & \mathbf{D} + \mathbf{D_p} \end{bmatrix}^{-1} \begin{Bmatrix} \mathbf{A_p} \\ \mathbf{B'_p} \end{Bmatrix} \Lambda \tag{17}$$

and the resulting transmitted forces, 11:

$$\begin{Bmatrix} \mathbf{N} \\ \mathbf{M} \end{Bmatrix} = - \begin{bmatrix} \mathbf{A} & \mathbf{B} \\ \mathbf{B} & \mathbf{D} \end{bmatrix} \begin{bmatrix} \mathbf{A}+\mathbf{A_p} & \mathbf{B}+\mathbf{B_p} \\ \mathbf{B}+\mathbf{B'_p} & \mathbf{D}+\mathbf{D_p} \end{bmatrix}^{-1} \begin{Bmatrix} \mathbf{A_p} \\ \mathbf{B'_p} \end{Bmatrix} \Lambda \tag{18}$$

With respect to the classical strain actuation theory, not only a bending moment and/or a normal stress, but also in-plane loads are transmitted to the structure. This, of course, can give rise to a complex kind of response that has to be examined in detail to prevent problems related to fatigue and delamination. Rigorously speaking, this formulation regards laminate panel only. Instead, a more detailed model should be realised for sandwich elements, taking into account the shear effects and their coupling to normal and bending stresses. However, as a first approximation it can be considered a starting point for both the types of structures.

Honeycomb plate

A sandwich panel is usually made of a honeycomb structure and two skin composite plates, so that the first supports most of the transverse shear, while the second absorbs almost all the bending stress. If the skin configuration is not symmetric, then a coupling is present between normal and bending actions, and the deformed shape results in a mix of the two kind of responses.
The first test article is referred to, consists of a large (1600×1300) honeycomb plate, clamped at the ends, manufactured at ONERA, Toulouse (F). The panel has a planar symmetry plane and is made up of 6 different fiberglass epoxy layers and a Nomex core. Honeycomb materials has higher stiffness in the normal plane (E_3) than the in-plane directions ($E_1 = E_2$) by 2 orders of magnitude. The in-plane shear constant (G_{12}) is negligible with respect to the other transversal characteristics ($G_{23} = G_{13}$); the values of these latter and E_3 are close to each other.
The feasibility of such an approach was verified through a modal analysis and a comparison with the experimental data provided by the French research center.[7] This result justified in some way the choice of applying the simplest S.A. model described before. The main idealisation consisted of considering the plate infinitely rigid in the transversal direction.

Dynamic response

ONERA panel was schematised with plane QUAD8 elements, by using MSC/NASTRAN code. The FEM model was made of 683 grids and 208 elements, up to a total of 3415 DOF's. The mesh was not uniform, because to have a more accurate description in the piezoceramics region, was preferred.

A numerical-experimental frequency response function comparison, confirmed the goodness of both the FEM and S.A. models adopted.[7] As a first step, the numerical dynamic response of the structure was analysed, due to both an acoustic pressure load system and piezoactuators devices, placed in different positions on the structure. The aim was to evaluate the feasibility of controlling the panel by using a small number of devices (6), to minimise the control effort.

Acoustic load

Three waves impinging on the panel from different angles were considered, fig.6.

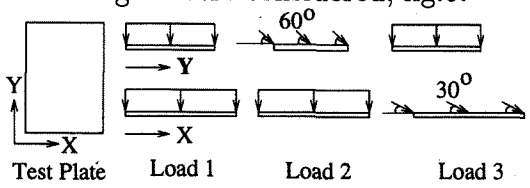

FIGURE 6: *Load sketch*

Each of them gave rise to a number of elementary not-phased loads so a complex excitation is generated. Namely, two pressure forces at a distance of Δd on the panel, induced by a wave incident with an angle α on the surface, present a time delay equal to:

$$\Delta\tau = \frac{\Delta d \cdot sin\alpha}{c} \qquad (19)$$

c being the sound speed. The global magnitude of such a load was set equal to 100 dB, defined as: $L_t = \sqrt{\sum_i L_i^2}$. Because of the asymmetrical nature of this kind of load, all the modes were expected to be excited. In fig.7 the comparison with the SWR's due to the piezo's and the primary load, is presented (V=100 V). The excitation levels are comparable in the different cases. Piezo distribution is reported in fig.8. No optimisation process was implemented to place the actuators. Really, a variety of different positions was chosen so to have a preliminary evaluation of the various locations goodness.

SWR control

An LMS based feed-forward control algorithm was referred to. The objective function was the radiated sound power, SWR.[19] This choice permits of reducing computational times, because instead of referring to a complex acoustic-structural coupled model, it needs the only information acquired on the structure to extrapolate the acoustic behaviour. It is strictly valid for a free field radiation and for rectangular plates only, but it can predict successfully the performance of an active control system for closed cavities. Particularly, the method treats of reproducing through the control actuation (secondary forces) a sound field equal and opposite to what is generated by the external disturbance (primary force). The formulation is closed, in the sense that the forces minimising the acoustic radiation are univocally determined for given structure, external load and actuator positions.

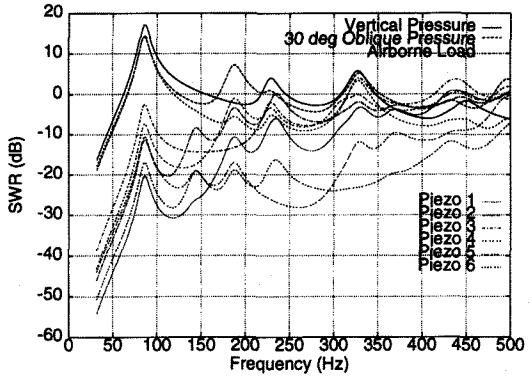

FIGURE 7: *SWR due to a combination of 3 acoustic disturbances (100 dB) and to piezo actuators (100 V)*

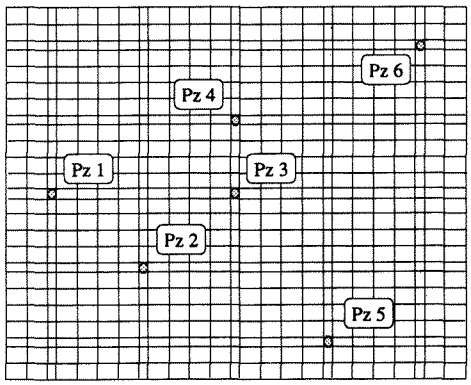

FIGURE 8: *Piezoelectrics location*

The result, in terms of frequency spectrum, is reported in fig.9. A good reduction was obtained all over the investigated range, with the exception of the first mode, where an attenuation close to 1 dB was verified. The applied method takes into account the voltage limit to be applied on each piezo device, in order

to give no rise to an excitation greater than the depolarisation voltage (in this case equal to 300 V). An index of the usefulness of each actuator is represented by the requested voltage spectra plot, fig.10. As it does appear, at the first mode only the fourth actuator was really working, while the others were well under the voltage limit. This simply means that the other control devices were ineffective at that frequency. For the other modes, all the piezoes were called to significative contributions, particularly the 5^{th} and the 6^{th}.

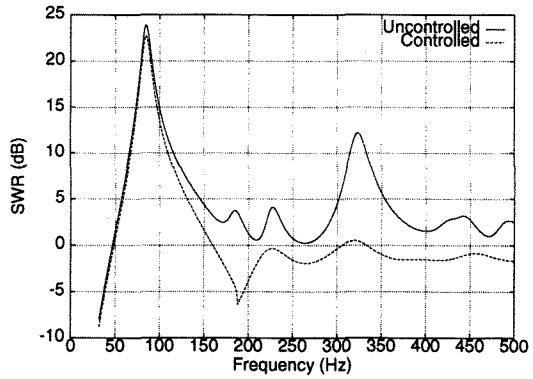

FIGURE 9: *Feed-forward control of an acoustic disturbance (airborne load 100 dB)*

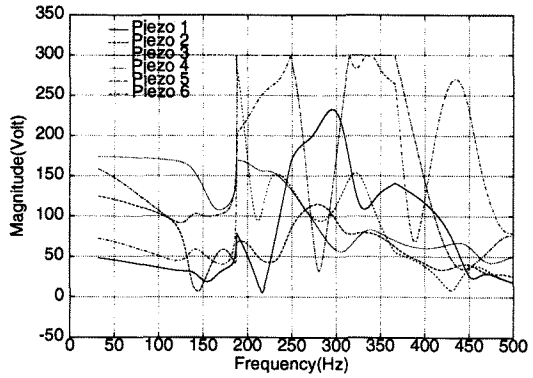

FIGURE 10: *Magnitude of the secondary forces paths (airborne load 100 dB)*

So, an up-dated distribution was defined (see fig.11) simply by locating four actuators at the center of the panel and leaving the 5^{th} and the 6^{th} in the former positions.
Control action produced the spectrum reported in fig.12 where it can be seen as an interesting improvement is reached, above all at the first frequency, while something is "lost" in the other regions.

Of course, to evaluate the adopted configuration is necessary to have a correct performance measure. This can be done by representing the covered area or the weight penalty: $\Delta A/A \simeq .31\%$ and $\Delta W/W \simeq .36\%$, that is to say, a really poor expense in terms of control effort. In spite of this, under a 100 dB magnitude external disturbance (equivalent to a resultant force of 4.16 N) six piezoactuators are able to balance its action by obtaining 3 dB SWR reduction at the first resonance frequency, where large vertical displacements are combined with a small strain field: i.e. the hardest working condition for piezoactuators.

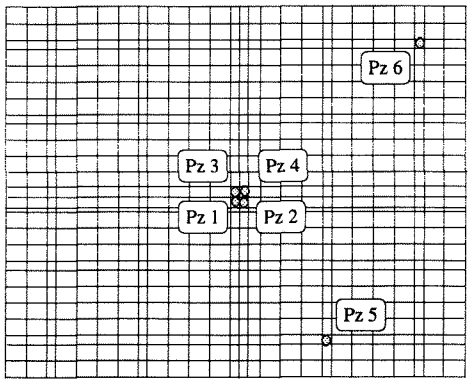

FIGURE 11: *Updated piezo location*

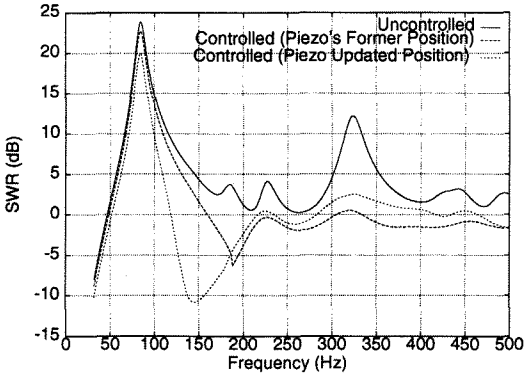

FIGURE 12: *Feed-forward control performance comparison for the two different piezo's location (airborne load, 100 dB)*

When the number of active devices is increased, or the covered area is enlarged, better results are achieved. Furthermore, it is evident as the actuators location plays a fundamental role in terms of control performance.

Curved framed composite plate

Most of helicopter panels do not have a flat surface. Dynamic properties depend strongly

on their geometry. Moreover, it could be convenient, or necessary, to model both trim and skin panels that make a unique structural element with peculiar characteristics; of course the presence of damping/elastic connectors should also be taken into account to effectively predict their behaviour.
A curved framed panel was designed and manufactured by DASA so to have a more realistic object to use as a reference point for industrial applications of active vibration/noise control on real aircraft. In this article, there is no reference to any experimental-numerical correlation, still on-going. With respect to the "real" test article, two major simplifications were introduced: no damping layer was inserted, and acoustic contributions (typical double-wall configuration) were not considered. FEM idealisation produced only an element to be regarded as a representative of that class of structural components and the reported results should be read only as qualitative.

Test article description

The test article scheme is reported in fig.13: it is made up of four elements:

- Trim panel;
- Stringers;
- Rubber mounts;
- Skin panel.

Lab specimen was entirely built up at DASA, where the experimental investigation (here not referred to) was carried out. The brief description following, is reported only for the sake of clarity. The air gap and the relative acoustic influence on the response were not simulated. Instead, the assumptions taken into account consider the structural transmission as dominating, compared to the acoustic path. This single-direction curved panel can be considered as being made up of a large panel with a flange on each side, characterised by a smaller curvature radius (370 vs 1195 mm). The skin panel is a sandwich plate made up of six layers on the external part, a honeycomb core (8 mm thick), and three layers inside, fig.13. Total thickness results as being about 9 mm. In the uncurved direction, five stringers are present at different stations: 2 $\sqsubset$ (external) and 3 $\mathbb{I}$-shaped (internal) beams. The trim panel, supported at the stringer locations by a certain number of rubber mounts, is unsymmetrical and unbalanced composite material made of 4 layers only, fig.13: it was considered the only able to radiate sound. Therefore, the action of the control system was thought to act on this structure.

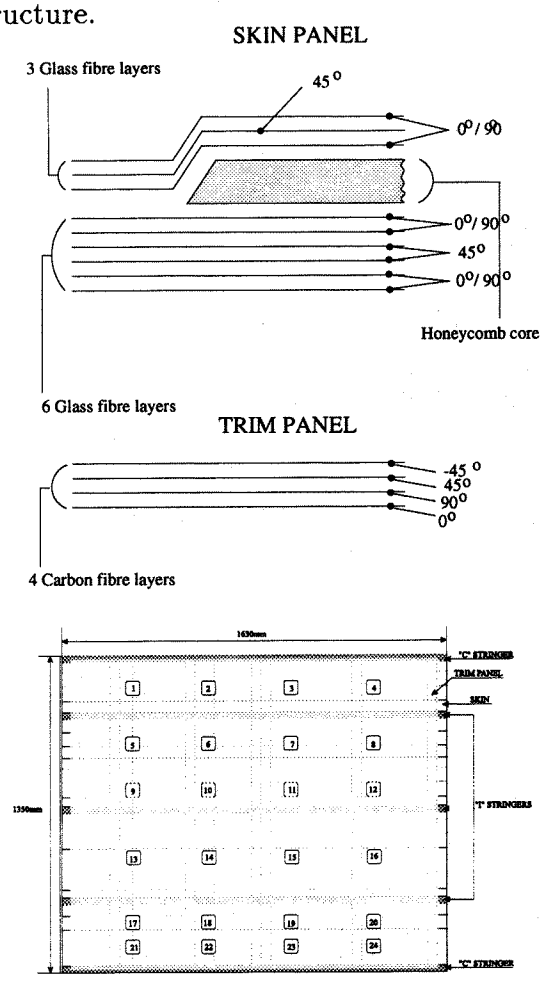

FIGURE 13: *DASA test article & piezo's location*

Taking advantage of the previous experiences on the flat panel, QUAD8 elements were chosen to model both the trim and the skin. They can also better follow the curvature of the structural elements under investigation because of mid-side nodes that allow discretisation of the elements through a 2nd-order spline. A non-homogeneous mesh, made of 80 BEAM, 15 ELAS, 120 BAR and 1640 QUAD8 elements for a total of 5371 GRID points and 26129 degrees of freedom was adopted. A single CQUAD8 was chosen to represent each active device. Again, no optimisation tool was used to define the placement; simply, piezo's were located in the region of maximum strain/curvature. Stringers were considered to have concentrated proper-

ties at the actual bonding lines. Elastic and mass elements were used to simulate rubber mounts (almost 5 g associated mass and 15% damping). Summarising, the model was realised through:

EL.	TRIM	SKIN	CON.	STR.
QUAD8	820	820	–	–
BAR	–	–	–	120
BEAM	–	–	–	80
RBAR	–	–	205	–
CELAS	–	–	15	–
CONM	–	–	30	–

EL.=Elements; CON.=Connectors; STR.=Stringers

Dynamic response

Numerical modal analysis[7] showed a low modal density in the investigated frequency range. Furthermore, each mode shape was seen to be trim-dominated, due to the high compliance of this element. All along the border, great flange distorsion could be observed. A system of 10 radial point forces was considered: in a first case, loads were applied on the stringers only; in a second case, some were placed on the trim so to check the effect of its direct excitation. As expected, vibration level was verified to be much higher in the second configuration, because of the high mobility associated to the trim. Nevertheless, it is interesting to evaluate the capability of the trim-placed piezo's to control an action on the stiffeners. The FRF's due to the different load distributions are reported in fig.14 and 15; the different order of magnitudes are evident.

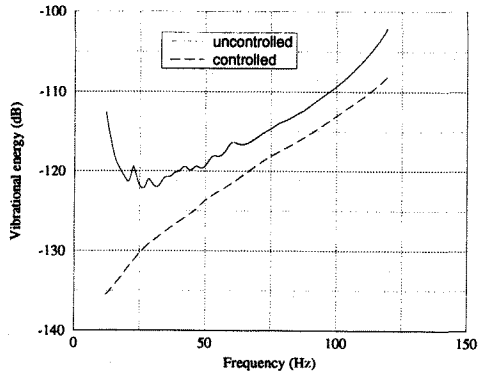

FIGURE 14: *Control on vibrational energy when forces act on the stringers*

In relative terms, the excitation on the stringers gave rise to high disturbance levels in the low and in the high frequency range, with a sort of "response gap" between 20 and 50 Hz. Furthermore, the response does not present evident resonance peaks, because the action on the stringers was not able to excite trim resonances. The mixed excitation, instead, produced a flat spectrum in the investigated range, but some peaks linked to the different resonant frequencies, appeared.

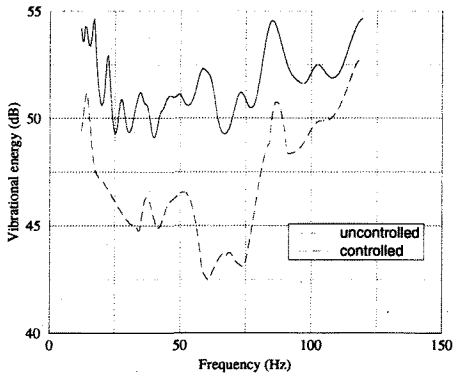

FIGURE 15: *Control on vibrational energy when forces act on the stringers and on the trim*

Vibrational energy control

Trim vibrational energy was assumed the cost function to be referred to. On this basis, only an action devoted towards the vibration suppression was moved; no effort was instead spent in modelling the structural response for a minimisation of the radiated sound field. If no cost factor is taken into account, a really optimistic performance is obtained. This would mean to refer to control actuators able to produce an effect in the measure as needed. Of course, this is not a reasonable assumption. More realistic data outcame as the piezo voltage limit (300 V) was considered. Both results are reported in figs 16 and 17.

With reference to the first type of load, a good result was obtained in the very low frequency range (10-25 Hz). Piezoes were able to give rise to a set of forces replying the quasi-static response. The diagram is a flat-type response, with a uniform reduction of 3-4 dB in the range 50-120 Hz, 5-10 dB in the range 25-50 Hz and up to 25 at 12 Hz. The reasons of this behaviour may be found in the high deformability level of the plate if compared to the stringers one. The little peaks associated to trim plate resonances are practically cancelled. A best performance is not

expected because the actuators should placed on the stiffening beams, instead: the same deformability of the plate gives rise to local deformation not involving the remaining part of the structure. This limit may be easily forecast also because of the minimal covered area ($\Delta A/A \leq 1\%$) and for the incremental weight factor ($\Delta W/W < 8\%$). In the end, it is reasonable to consider as the control effort factor never exceeds 0 in the investigated range. This assures that piezo's are not able to produce a dynamic deformed shape as the external load actually does. To improve the results, at least two ways could be pursued: placing more actuators and optimising their placement (e.g. putting them on the stringers).

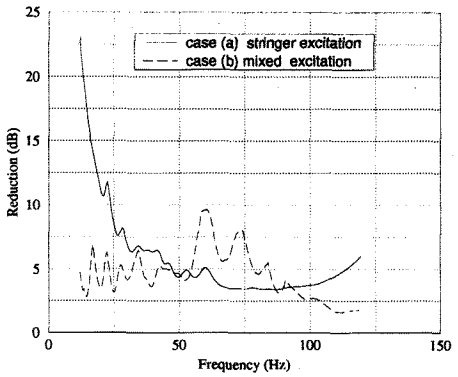

FIGURE 16: *Control performance for the different load conditions*

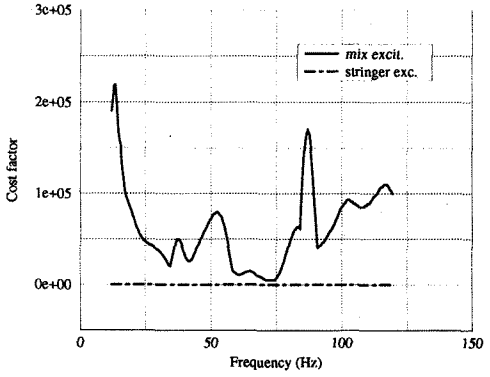

FIGURE 17: *β factor for both external loads*

For the second load-type, results were quite different: above all, absolute response was very higher, because some forces are placed on the trim; hence, a good vibrational response is produced, fig.15. Apart of some peaks, many resonances vanish; this is an effect of the piezo placement, of course, able to control only some mode shapes. Anyway, reduction is again assessed between 3 and 10 dB, also if on a wider range (up to 100 Hz). Something changed as frequency grows, and this would be linked to some stringers eigenfrequencies approaching. Cost factor, fig.17 is heavily involved and reaches high values, to asses the "in-principle" capability of the actuators to control those particular modes, for that load and configuration. As a general conclusion, it may be stated that, for the used configuration, piezo actuators were not able to produce better reductions for their distribution and number.

Placement quality

The electric active power expense is linked to the real part of the ratio between squared voltage and electrical impedance:

$$W_{exp} = \mathbf{Re}(V^2/Z) \tag{20}$$

It may be useful to show the behaviour of the averaged requested voltage as representative of the control cost (it is simply to consider that, being $Z=R+i\cdot I$ and $R \gg I$, for piezoes, $V^2_{avg} \simeq W_{avg}$):

$$W_{avg} \simeq V^2_{avg} = \frac{\sum_i V_i^2}{nV^2_{max}} \leq 1 \tag{21}$$

Where V_i is the voltage applied to each actuator, V_{max} the voltage limit and n the number of piezoes. The result is reported in fig.18 for the mixed excitation only, that provided the most interesting results.

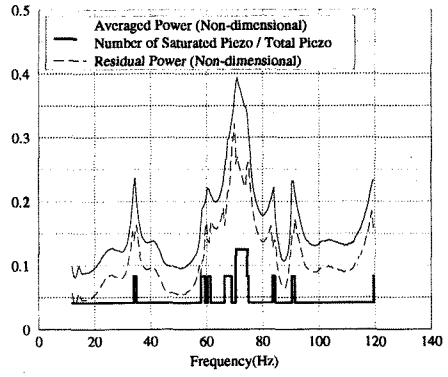

FIGURE 18: *Power expended by each actuator & its different contributions*

As it can be seen, active devices absorbed the maximum averaged power in the same

range where the cost factor was the lowest; as a general statement, piezo's may be said to work here in a more homogeneous way that elsewhere in the investigated frequency range. Also the value of W_{avg} may be seen to be always less or equal to 0.4: this points out again that the chosen placement was really not optimised (the greater this value, the greater the piezo's contribution to the control effort).
Referring again to fig.18, the number of saturated piezo's is reported as a non-dimensional step function, that is referred to the total involved piezoceramics. They are defined as the devices that work around the maximum allowable voltage (300 V) with a tolerance of 10 %. If the averaged expended power is referred to, as defined in the equation 21, an interesting consideration may be extracted. In fact, the aforementioned equation may be expressed as:

$$W_{avg} \simeq \frac{\sum_{i=1}^{n_{ps}} V_i^2}{nV_{max}^2} + \frac{\sum_{i=n_{ps}+1}^{n} V_i^2}{nV_{max}^2} \qquad (22)$$

where n_{ps} is the number of saturated piezoes (as defined beforehand). By considering that V=300 V ($\Rightarrow$ V=V_{max}), when a piezo works in saturation, it follows:

$$W_{avg} \simeq \frac{n_{ps}}{n} + \frac{\sum_{i=n_{ps}+1}^{n} V_i^2}{nV_{max}^2} \qquad (23)$$

For the sake of simplicity, it can be written as:

$$W_{avg} \simeq \frac{n_{ps}}{n} + W_{res} \qquad (24)$$

W_{res} is linked to the "degree of use" of the ceramic devices different from the saturated ones.

In fig.18 the difference between the two curves W_{res} normalised is also reported. The greater this value, the more the effort is distributed among all the involved active devices and better is the placement adopted (at each frequency).
It may be interesting to express the averaged level of each non-saturated piezo. It is given by:

$$W_{avg,res} = W_{res} \cdot \frac{n}{n - n_{ps}} \qquad (25)$$

The corresponding value navigates around 15%. All over the investigated frequency range, there is at least one piezo working in saturation. On the other hand, the maximum number reaches 3 in the range between 70 and 75 Hz.

Conclusions

An isotropic-based S.A. model has been demonstrated to be able to predict in a suitable way the transmitted strain field by piezoceramics to honeycomb plates.

A dedicated model has been presented with reference to unsymmetrical and to unbalanced composites. Shear effects were not taken into account in both cases, and this can represent the next step inside the on-going research.

Two different applications have been presented, relative to a flat and a curved framed plate, respectively. Test articles were manufactured at ONERA, Toulouse and at DASA, Munich, where the experimental investigations were carried out. Here only numerical results have been reported.
Referring to the flat plate, interesting performances were obtained by using only a little number of small ceramic devices (coverage area or weight incremental factor less than 1%). Problems were found in the low frequency range that is the worst working condition for piezoceramic patches. This kind of devices transmits a stress field: hence the energy is linked to the strain associated field.
For large structural elements, great displacements with low strain levels are expected. Anyway, this problem was minimised by referring to a more suitable devices placement.

The curved framed panel confirmed enough the obtained results. Particularly, two load configurations (point force systems) were studied. Referring to this test article, averaged expended power was calculated and it demonstrated to be a good reference point for the placement optimisation.
In spite of the high deformability of the panel, a good vibration reduction was obtained overall the investigated frequency range. Again, the bad placement and the poor coverage area factor revealed to be very important factors in the control system performance.

As a general conclusion, it can be asserted that the most important parameters for a given structure, inside the numerical design of a control system may be summarised as follows: numbers ad placement of active elements (both sensors and actuators); control algorithm; type of external loads; suitable optimisation indexes. Particularly, it has to be clearly expressed "what" and "how" we must control to affirm that the actuators and sensors are "nicely" placed.

Acknowledgements

The authors would like to thank Prof. L.Lecce, Dept. of Aeronautical Engineering at Univerity of Naples, for his precious contribution and suggestions; Mrs. S.Pauzin and Mr. F.Simon, CERT-ONERA, Toulouse, as well as Mr. G.Niesl and his staff, Eurocopter Deutschland, Munich, for their collaboration and useful support in the realisation of the complete work inside RHINO program, by which this article descends; Mr. M.Maggiore, Agusta, Varese, that showed a continuous interest in this research.

References

[1] Crawley E.F., de Luis J., "Use of Piezoelectric Actuators as Elements of Intelligent Structures", AIAA Journal, Vol. 25, Nr. 10, Oct.1987.

[2] Dimitriadis E.K. et al., "Piezoelectric Actuators for Distributed Vibration Excitation of Thin Plates", trans. ASME, Journal of Vibration and Acoustics, Vol.113, Jan.1991.

[3] Wada B.K. et al., "Adaptive Structures", Journal of Intelligent Materials and Structures, Vol.1, N.2, 1990.

[4] Fuller C.R., "Recent Developments in Active Control of Vibration", Nordic Conf. on Vehicle and Machine Vibrations, Stockholm (S), Sep.1994.

[5] Concilio A. et al., "A Comparison of Different Methodologies for Aircraft Internal Noise Reduction by Active Vibration Control", 3rd Int.Cong. on Air- and Structure-Borne Sound and Vibration, Montreal (CAN), Jun.1994.

[6] Lecce L., Concilio A., "Actuation of Thin-Walled Beams by Distributed Piezo-Actuators", Actuator '94 Conf., Bremen (D), Jun.1994.

[7] De Vivo L., Concilio A., "Numerical Studies of a Piezoceramic-Based System on Typical Helicopter Panels" CEC Report, CIRA-TR-96-025, CIRA, Capua-CE (I), Feb.1996.

[8] AA.VV., "RHINO Work-programme", IMT-CEE Project, 1992.

[9] Lecce L. et al., "Active Control of Noise and Vibration on Panels with a Simple Self-Adaptive System using Distributed Piezoelectric Devices", 2nd ATA Int.Conf., Bologna (I), Oct.1992.

[10] Ross C., "Active Sound Control: the Benefits in Passenger Cabins", Nordic Conf. on Vehicle and Machine Vibrations, Stockholm (S), Sep.1994.

[11] Paonessa A. et al., "Active Control of Sound in ATR42", Noise-Con '93, May 1993.

[12] Pauzin S., Simon F., "Active Control of the Radiation of a Honeycomb Flat Panel (Probative Tests)", CEC Report RH6CERT-ONERA2T CERT-ONERA-DERMES Toulouse (F), Jan.1995.

[13] Roozen N.B., "Quiet by Design: Numerical Acousto-Elastic Analysis of Aircraft Structures", Ph. D. Thesis, Tecnische Universiteit Eindhoven (NL), May 1992.

[14] Emborg U., "Application of Active Noise Control in Saab 340 and Saab 2000", Nordic Conf. on Vehicle and Machine Vibrations, Stockholm (S), Sep.1994.

[15] AA. VV., "IDEA PACI Work-programme", IMT-CEE Proposal, 1995.

[16] Concilio A. et al., "Active Noise Control on Plates and Double-Wall Partitions using Discrete Piezoelectric Devices", DGLR/AIAA XIV Aeroacoustic Conf., Aachen (D), May 1992.

[17] Concilio A., "Cabin Noise Active Control through Piezoelectric Actuators Bonded on the Structure", Ph. D. Thesis, Univ.of Napoli (I), Nov.1995 (in Italian).

[18] Ochoa O.O., Reddy N., "Finite Element Analysis of Composite Laminates", Kluwer Academic Publishers, Dordrecht (NL), 1994.

[19] Nelson P.A., Elliott S.J., "Least Squares Approximation to Exact Multiple Point reproduction", ISVR Memorandum Nr. 683, Aug.1988.